European Journal of Neurology

european journal of neurology
the official journal of the european academy of neurology

ORIGINAL ARTICLE OPEN ACCESS

Novel SCN4A Variants Associated With Myalgic Myotonic Disorder or Paramyotonia

Vesa Periviita[1] | Roope Männikkö[2] | Manu Jokela[3,4] | Richa Sud[2] | Michael G. Hanna[2] | Bjarne Udd[5,6] | Johanna Palmio[5]

[1]Department of Neurology, Tampere University Hospital, Tampere, Finland | [2]UCL Queen Square Institute of Neurology, Department of Neuromuscular Disease, London, UK | [3]Neurocenter, Turku University Hospital, Turku, Finland | [4]Clinical Neurosciences, University of Turku, Turku, Finland | [5]Neuromuscular Research Center, Tampere University and University Hospital, Tampere, Finland | [6]Folkhälsan Research Center, Helsinki, Finland

Correspondence: Vesa Periviita (vesa.kari@fimnet.fi)

Received: 19 January 2025 | **Revised:** 12 March 2025 | **Accepted:** 3 April 2025

Funding: This work was supported by the Tampere University Hospital Support Foundation, Päivikki and Sakari Sohlberg Foundation, Finnish Medical Foundation, 7629, Paulo Foundation, and Maire Taponen Foundation.

Keywords: channelopathies | muscular diseases | myalgia | observational study

ABSTRACT

Background: This study aimed to determine the role of five new rare *SCN4A* variants suspected to cause paramyotonia or myotonic disorder.

Methods: Ten patients from seven families underwent clinical, neurophysiological, imaging, and muscle biopsy examinations. Genetic studies were performed with targeted sequencing of all known myopathy genes. Functional changes resulting from these variants were studied with HEK293T cells, by using a whole-cell patch clamp.

Results: Five *SCN4A* variants were identified: c.662 T > C p.(F221S), c.2143G > A p.(A715T), c.4352G > A p.(R1451H), c.3610 A > G p.(N1204D), and c.4255 T > C, p.(F1419L). Patients had exercise- and/or cold-induced myalgia, muscle stiffness or cramping, and varying degrees of muscle weakness. On examination, some but not all patients had percussion myotonia or findings compatible with paramyotonia. One patient with the A715T variant also had eyelid myotonia. The patient with the F221S variant had ptosis, weakness in hip flexion, and mild muscle hypertrophy in the calves. EMG showed myotonic discharges in all the patients examined except for the patient with N1204D. Electrophysiological exercise tests demonstrated results compatible with the Fournier pattern in six patients. All but the N1204D variant showed gain-of-function features upon functional expression.

Conclusions: The clinical and genetic findings suggested that all five variants were pathogenic, whereas functional data did not confirm association with myotonia for N1204D. Our results expand the mutational spectrum of the *SCN4A* gene. The reported variants should be considered in patients with paramyotonia, or in patients with exercise-induced myalgia or muscle cramping and who demonstrate myotonia in EMG.

1 | Introduction

The *SCN4A* gene encodes the pore-forming α-subunit of the voltage-gated $Na_v1.4$ channel expressed in skeletal muscle cells [1]. It locates on the muscle cell membrane and on the membranes of T-tubules [2]. Muscle depolarization activates these channels, which triggers action potentials in the muscle cells. Voltage-gated sodium channels are composed of four homologous repeats, each composed of a voltage-sensing domain (VSD) and a pore domain. The four pore domains join to form a single central sodium-conducting pore. Depolarization triggers activation of VSDs that leads to the opening of the ion-conducting pore. The most C-terminal VSD activates slower than the other VSDs and drives fast inactivation that follows

channel opening. Inactivation limits sodium inflow and the action potential [3].

Skeletal muscle channelopathies are caused by gene variants that alter the function of encoded ion channels expressed in muscle cells. They result in changes in cell membrane excitability, causing various clinical symptoms [4]. The reported number of such causative *SCN4A* variants is over 70 [5] and increasing. Sodium channel channelopathies affecting skeletal muscle include hypokalemic [6] and hyperkalemic periodic paralyzes [7], paramyotonia congenita [8], sodium channel myotonia [9], and myalgic stiffness without significant myotonia [10]. These conditions are dominantly inherited. $Na_v1.4$ variants found in the patients show gain-of-function (GoF) features that may result in increased excitability and myotonia or persistent depolarization and paralysis. Recently, and more rarely, recessive $Na_v1.4$ loss-of-function (LoF) variants have been associated with congenital myasthenia [11] and congenital myopathy [12].

Musculoskeletal pain is a frequent complaint [13]. Myalgia may be a presenting symptom in skeletal muscle diseases as well. Myalgia is a major complaint in myotonic dystrophy type 2 (DM2) [14]. Patients with myotonia congenita or sodium channel myotonia may suffer from painful myotonia [15, 16]. A specific *SCN4A* variant p.(A1156T) causes myalgic syndrome together with muscle stiffness and muscle cramping [10, 17]. A rare CACNA1S variant p.(E965Q) was associated with a myopathy with severe myalgia and unusual muscle hypertrophy [18].

We encountered seven families whose members complained of myalgia and muscle stiffness provoked by physical exercise or cold, or both. They also reported varying muscle weakness. Extensive investigations revealed four previously unreported *SCN4A* variants. One variant was already reported in the literature [19] and was suspected to cause skeletal muscle channelopathy at the time. This study aimed to determine whether these five *SCN4A* variants were responsible for the suspected channelopathy in these studied patients.

2 | Patients and Methods

2.1 | Clinical Examinations

The study comprised ten patients from seven families (Figure 1). Family history and medical records were reviewed. Clinical neuromuscular examination included detailed manual muscle strength assessment and myotonia testing by muscle percussion, handgrip, and eyelid closure. F2 II:1 lived in Finland but was originally from Kosovo. F7 II:1 was British. All other study patients were Finnish.

2.2 | Neurophysiological Studies

Standard neurography and needle electromyography (EMG) were conducted on all study patients. The proximal and distal parts of at least one upper and one lower limb were examined.

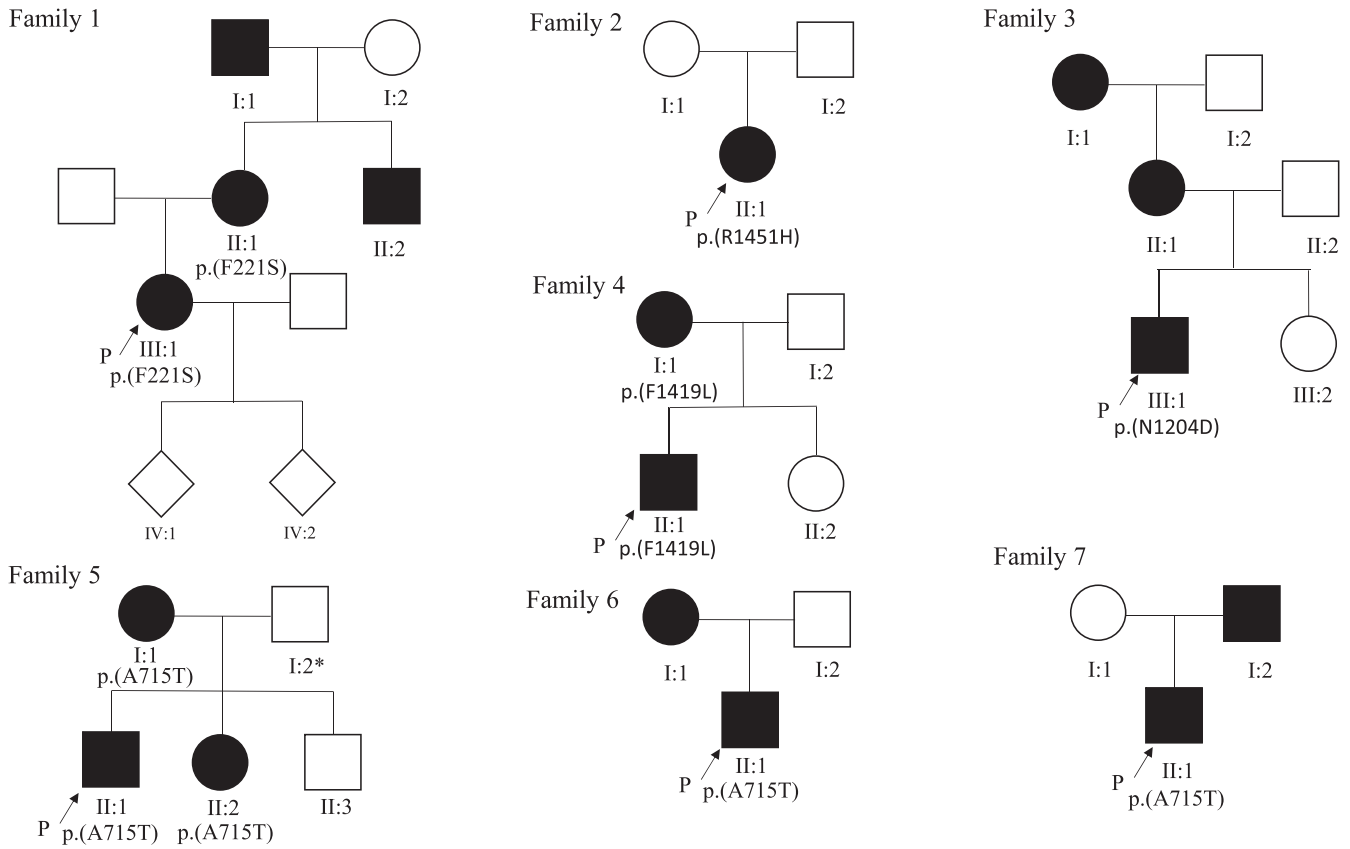

FIGURE 1 | Pedigrees. Pedigrees of the study families. Affected individuals are represented with shaded symbols. F5 I:2 was the only individual who underwent genetic testing and did not have a pathogenic *SCN4A* variant. He is marked with an asterisk. All others who were tested had a pathogenic variant. These variants are superimposed in the figure. F1 IV:1 and F1 IV:2 were underage. Their sex is not specified here.

Electrophysiological exercise testing was performed by using a protocol described by Fournier, consisting of short (10–12 s) and long (5 min) exercise tests [19, 20]. Abductor digiti minimi (ADM) and extensor digitorum brevis (EDB) muscles were examined in the short exercise test (SET), and the ADM muscle in the long exercise test (LET). SET was also performed after cold exposure. The ADM muscle was cooled by applying an ice bag on the muscle for 7 minutes. The temperature of the skin after cooling was usually 18°C–20°C. The target temperature was achieved in all cooling tests. Compound muscle action potential (CMAP) amplitude was the parameter measured in the exercise tests. Normal ranges and EMG patterns described by Fournier and colleagues were applied when interpreting the results of SET, LET, and SET with cold provocation [19, 20]. Percentages regarding CMAP exercise test results refer to pre-exercise values. The exercise testing, always comprising SET, LET, and SET with cold provocation, was performed in F1 III:1, F3 III:1, F4 II:1, F5 II:1, F5 II:2, and F7 II:1.

2.3 | Muscle Biopsy and Histology

At least one muscle biopsy was obtained from probands of the families F1, F2, and F6. The target muscle of F1 III:1 was m. vastus lateralis, of F5 II:1 m. deltoideus, and of F3 III:1 both m. vastus lateralis and m. deltoideus. Standard histology and histochemical stainings [21] were performed, including hematoxylin and eosin, modified Gomori trichrome, periodic acid Schiff (PAS), nicotinamide adenine dehydrogenase (NADH), combined succinate dehydrogenase–cytochrome oxidase, and myosin heavy chain double staining [22].

2.4 | Muscle Imaging

Axial MRI sections of the lower limbs included T1- and T2-weighted sequences, and short tau inversion recovery (STIR) sequence. Probands F1 III:1, F3 III:1, and F5 II:1 were examined by MRI.

2.5 | Molecular Genetics

Genomic DNA was isolated from peripheral blood samples by using standard methods. The genetic analysis was performed by using a targeted next-generation sequencing (NGS) gene panel MYOcap v5 or MYOcap v6 targeting the exons and intronic borders of 328 and 339 myopathy genes [23]. The genetic analysis of F7 II:1 was also performed by using a targeted NGS gene panel used in the trip UK.

2.6 | Functional Studies

Mutations were introduced to *SCN4A* by using the QuikChange Mutagenesis Kit (Agilent) and confirmed by sequencing of the whole gene. *SCN4A* plasmids were transfected into HEK293T cells by using Lipofectamine2000 together with a plasmid encoding green fluorescent protein as a transfection reporter. Single cells with green fluorescence were patched with electrodes filled with intracellular solution containing (in mM) NaCl (5), CsCl (145), EGTA (10), and HEPES (10) with pH 7.4. The extracellular solution contained (in mM) NaCl (145), KCl (4), $MgCl_2$ (1), $CaCl_2$ (2), and HEPES (10) with pH 7.4. Following the obtaining of whole-cell configuration, the cell was allowed to settle for 10 min while observing the stabilization of the currents. Currents were sampled at 10 kHz by using Clampex software, Digidata 1550A converter, and amplified by using Axopatch 200B Amplifier (all Molecular Devices). Series resistance was compensated $\geq 75\%$ keeping the voltage error below 5 mV. Voltage protocols are described in legends and in Luo et al. 2018 [24]. The $-P/4$ protocol was used to subtract leak and capacitive currents in all but slow inactivation protocols. The holding voltage was −80 mV except for the closed state inactivation protocol where it was −100 mV. Voltage dependence of activation and inactivation was fit with the Boltzmann equation, and the time course of onset and recovery from inactivation with the exponential equation. Variants were expressed at different timepoints with wild-type channels expressed in each transfection to control for expression and channel properties. Data are expressed as mean ± standard error of mean. Statistical comparisons were performed by using one-way or Kruskal–Wallis ANOVA, with Bonferroni or Dunn tests, respectively, to compare the means.

2.7 | Standard Protocol Approvals, Registrations, and Patient Consents

This study was approved by the Research Ethics Committee of the Wellbeing Services County of Pirkanmaa. The study was performed according to the Declaration of Helsinki. Written informed consent from all participants was obtained since the study was performed in the context of research.

3 | Results

3.1 | Family 1

3.1.1 | F1 III:1

The proband (Table 1) was in her late twenties. She had muscle stiffness in her fingers and lower limbs during her first pregnancy several years earlier. She also had myalgia and muscle weakness in her lower limbs. Stiffness and myalgia were provoked by cold and physical exercise, and occasional muscle cramping occurred. Symptoms diminished substantially after her pregnancy but exacerbated again during her second pregnancy and persisted after delivery. She required occasional sick leave. Her mother, uncle, and grandfather complained of muscle stiffness and myalgia. Muscle weakness was not recorded. The patient had two asymptomatic children.

On examination, her calves were mildly hypertrophic. There was no clinical myotonia. The margin of the left upper eyelid was lower compared to the right. Hip flexion was 4/5, but otherwise, muscle strength was normal. EMG demonstrated increased insertional activity, myotonic discharges, and polyphasic motor unit potentials. Electrophysiological exercise tests showed a 95% increase in amplitude in the long exercise test before slowly decreasing. These findings were compatible with Fournier pattern IV. The muscle biopsy and CK values were normal. Muscle MRI of the lower limbs was normal. Genetic testing of myotonic

TABLE 1 | Clinical data of the families F1–F4.

Family member	F1 II:1	F1 III:1	F2 II:1	F3 III:1	F4 II:1
Sex/age	F/40–64	F/18–39	F/40–64	M/40–64	M/18–39
Age at onset	18–39	18–39	40–64	40–64	Childhood
Muscle weakness	Proximal lower limbs	Lower limbs	No	All limbs, more severe in the lower limbs	Upper limbs
Other symptoms	Exercise- and cold myalgia and stiffness	Exercise- and cold-induced myalgia and stiffness	Exercise-induced muscle cramping, myalgia	Exercise-induced myalgia and stiffness, muscle cramping	Exercise-induced stiffness and muscle cramping, cold-induced stiffness
Clinical findings	n.a.	Weakened hip flexion, marginal ptosis, and mild hypertrophy in the calves	Normal	Normal	Normal
CK level	Normal	Normal (59–114)	n.a.	Normal	n.a.
EMG	Myotonic discharges	Increased insertional activity, myotonic discharges, and polyphasic MUPs	Myotonic discharges	Polyphasic motor unit potentials	Myotonic discharges
Electrophysiological exercise testing	n.a.	LET compatible with Fournier pattern IV	n.a.	SET at room temperature and with cold provocation compatible with Fournier pattern I	Fournier pattern III
Muscle biopsy	n.a.	Normal	n.a.	Basophilic degeneration and vacuoles	n.a.
MRI of the lower limbs	n.a.	Normal	n.a.	Normal	n.a.
Genetics	Heterozygous *SCN4A* c.662 T > C p.(F221S)	Heterozygous *SCN4A* c.662 T > C p.(F221S)	Heterozygous *SCN4A* c.4352G > A p.(R1451H)	Heterozygous *SCN4A* c.3610A > G p.(N1204D)	Heterozygous *SCN4A* c.4255 T > C, p.(F1419L)

Note: Normal range of CK for male subjects aged 18–49 years was 50–400 U/L, and for male subjects aged over 49 years 40–280 U/L. Normal range of CK for female subjects aged over 17 years was 35–210 U/L. Precise readings of CK are given when available. Genetic testing was not performed with other family members at the time this article was written, except for F4 1:1 who had similar symptoms as F4 II:1 and the same heterozygous *SCN4A* variant.
Abbreviations: CK, creatine kinase; EMG, electromyography; F, female; LET, long exercise test; M, male; MUP, motor unit potentials; n.a., not available; SET, short exercise test.

dystrophy Type 1 (DM1) and DM2, and myotonia congenita were negative. MYOcap gene panel revealed a previously unreported heterozygous *SCN4A* variant c.662 T > C p.(F221S).

3.1.2 | F1 II:1

The mother complained of muscle weakness in her lower limbs and had difficulty climbing stairs. Symptoms began during her pregnancy in her early adulthood. Symptoms exacerbated when hormone therapy after menopause began. She had myalgia and muscle stiffness in her lower limbs, and muscle stiffness in her fingers. Stiffness and myalgia were provoked by cold and physical exercise. CK was normal. EMG showed myotonic discharges. Genetic testing of DM1 was negative. Segregation studies revealed a heterozygous *SCN4A* variant c.662 T > C p.(F221S).

3.2 | Family 2

3.2.1 | F2 II:1

A middle-aged female had muscle cramping in her calves when she approached middle age. Cramping was provoked by physical exercise, and possibly by cold. For years she had muscle aching, which had led to a diagnosis of fibromyalgia. Clinical examination was unremarkable. EMG showed myotonic discharges. Her parents were asymptomatic, although her mother had weakness in her lower limbs at advanced age. A previously unreported heterozygous *SCN4A* variant c.4352G > A p.(R1451H) was discovered.

3.3 | Family 3

3.3.1 | F3 III:1

A male in his early middle age presented with exercise-induced myalgia, muscle stiffness, muscle weakness, and muscle cramping. Symptoms were more prominent in the lower limbs. He was able to walk only 200–300 m without pausing. Clinical examination and CK were normal. EMG showed unspecific polyphasic motor unit potentials. Electrophysiological exercise testing demonstrated progressive decrement in SET with m. ADM. Decrement was up to 37% and more severe with cold provocation, being up to 59%. Muscle biopsy demonstrated basophilic degeneration in some fibers and vacuoles apparent on modified Gomori trichrome staining. MRI of the lower limbs showed a reduction in the subcutaneous adipose tissue. Genetic studies identified a previously unreported heterozygous *SCN4A* variant c.3610A > G p.(N1204D). The patient was diagnosed with paramyotonia congenita. His mother also had muscle stiffness and exertional muscle cramping since early adulthood.

3.4 | Family 4

3.4.1 | F4 II:1

A young male presented with cold-induced muscle stiffness in the upper limbs and facial muscles. He had difficulty opening his eyes in the cold. Exercise repetition provoked muscle cramping and difficulty in opening his hands after clenching his fists. The symptoms began already in childhood. Neurological examination was normal without clinical myotonia. EMG demonstrated myotonic discharges in all the muscles examined. Electrophysiological exercise testing was compatible with Fournier pattern III. Short exercise test with m. EDB induced immediate increments up to 53% after the first and second exercises. These increases quickly resolved. In LET, immediate increment of +33% was followed by almost complete recovery 10 min after exercise. CMAP amplitude slowly and steadily decreased, being −10% compared with the pre-exercise value at the end of the examination, and a 32% decrease from the peak value. The patient was diagnosed with paramyotonia congenita. A previously unreported heterozygous *SCN4A* gene variant c.4255 T > C p.(F1419L) was discovered. His mother had similar symptoms and the same heterozygous *SCN4A* variant.

3.5 | Family 5

3.5.1 | F5 II:1

The proband (Table 2) in his late twenties was never able to do push-ups properly. He had muscle aching and muscle stiffness in the upper limbs already in adolescence, both provoked by physical exercise and cold. He was examined complaining of muscle weakness in the upper limbs when he was a younger adult. At the time, burning myalgia occurred when he kept his arms lifted. Gradually, muscle weakness resolved spontaneously and the more prominent muscle weakness disappeared after some weeks.

Percussion myotonia was elicited on clinical examination. CK was normal. EMG showed myotonic discharges in all muscles examined, both in the proximal and distal muscles. Electrophysiological exercise testing showed an increase in amplitude by 39% in LET. The findings were interpreted to be compatible with Fournier pattern III. Muscle biopsy from m. deltoideus showed a slightly increased number of internal nuclei. Muscle MRI of the lower limbs demonstrated marginally increased fatty degeneration in soleus muscles. Brain MRI was normal. Genetic testing excluded facioscapulohumeral muscular dystrophy (FSHD) and myotonic dystrophies, as well as pathologic variants in *ANO5* and *SGCA*. MYOcap gene panel revealed a heterozygous *SCN4A* variant c.2143G > A p.(A715T) which has been previously reported once [19]. Regular lamotrigine medication had a positive effect.

3.5.2 | F5 II:2

The sister had myalgia and muscle stiffness, both provoked by physical exercise and cold. Cold also caused difficulties to speak properly. Repeated clenching of fists provoked stiffness, and the motion became slow, consistent with paramyotonia. Percussion myotonia was elicited in both thenar eminences. CK was normal. EMG showed myotonic discharges in m. extensor digitorum and increased insertional activity in the muscles of the upper limbs. Electrophysiological exercise testing with cold provocation induced up to −43% decrement, being

TABLE 2 | Clinical data of the families F5–F7.

Family member	F5 I:1	F5 II:1	F5 II:2	F6 II:1	F7 II:1
Sex/age	F/n.a.	M/18–39	F/18–39	M/40–64	M/18–39
Age at onset	n.a.	Adolescence	Adolescence	n.a.	18–39
Muscle weakness	No	Proximal upper limbs	No	No	Episodic with varying severity, accompanied by hypokalemia
Other symptoms	Exercise- and cold-induced myalgia and stiffness	Exercise- and cold-induced myalgia and stiffness	Exercise-induced myalgia and stiffness, cold-induced stiffness and difficulties to speak properly	Cold caused stiffness and difficulties to speak properly	Muscle stiffness
Clinical findings	n.a.	Percussion myotonia in thenar eminence	Percussion myotonia in thenar eminence	Muscle hypertrophy	Eyelid myotonia, muscle hypertrophy
CK level	n.a.	Normal (85)	Normal (86)	Normal	n.a.
EMG	Myotonic discharges	Myotonic discharges	Myotonic discharges	Increased insertional activity, myotonic discharges	Myotonic discharges
Electrophysiological exercise testing	n.a.	Fournier pattern III	SET with cold provocation compatible with Fournier pattern II	n.a.	Marked decrements in LET and in SET with cold provocation
Muscle biopsy	n.a.	Myopathic	n.a.	n.a.	n.a.
MRI of the lower limbs	n.a.	Marginally increased fatty replacement in soleus muscles	n.a.	n.a.	n.a.
Genetics	Heterozygous *SCN4A* c.2143G > A p.(A715T)	Heterozygous *SCN4A* c.2143G > A p.(A715T)	Heterozygous *SCN4A* c.2143G > A p.(A715T)	Heterozygous *SCN4A* c.2143G > A p.(A715T)	Heterozygous *SCN4A* c.2143G > A p.(A715T)

Note: Normal range of CK for male subjects aged 18–49 years was 50–400 U/L, and for male subjects aged over 49 years 40–280 U/L. Normal range of CK for female subjects aged over 17 years was 35–210 U/L. Precise readings of CK are given when available. Genetic testing was not performed with other family members at the time this article was written, except for F5 I:2 who was asymptomatic and negative for known pathogenic SCN4A variants.
Abbreviations: CK, creatine kinase; EMG, electromyography; F, female; LET, long exercise test; M, male; MUP, motor unit potentials; n.a., not available; SET, short exercise test.

compatible with Fournier pattern II. Segregation studies identified a heterozygous *SCN4A* variant c.2143G > A (p.A715T). The third sibling and the father of all the siblings were asymptomatic. The father was negative for *SCN4A* variant c.2143G > A p.(A715T).

3.5.3 | F5 I:1

The mother reported similar symptoms as her two symptomatic children EMG showed myotonia. She had a heterozygous *SCN4A* variant c.2143G > A p.(A715T).

3.6 | Family 6

3.6.1 | F6 II:1

A male approaching his middle age complained of myalgia and numbness in his arms. He had difficulty releasing his grip and speaking properly when cold and showed large muscles on inspection. EMG revealed increased insertional activity and myotonic discharges. CK was normal. His mother had similar symptoms. Genetic testing identified a heterozygous *SCN4A* variant c.2143G > A p.(A715T).

3.7 | Family 7

3.7.1 | F7 II:1

A male in his early thirties had an episode of mild muscle weakness after sports activity. This resolved spontaneously in a few hours. A few years earlier, he developed an episode of severe arm and leg weakness after a viral infection. Potassium level was 2.4 IU/L. He received intravenous potassium, which improved his state. He noticed stiffness when rising from a chair. Examination revealed eyelid myotonia and muscle hypertrophy. EMG demonstrated myotonic discharges. SET was normal at room temperature, but SET with cold provocation induced a marked decrement. The LET induced a decrease in amplitude by 49% from the peak value. Genetic testing identified a heterozygous *SCN4A* variant c.2143G > A p.(A715T). The father had hypokalemia with associated muscle weakness as well but was not available for genetic testing.

3.8 | Functional Analysis

The variants identified in this study affect residues conserved among Na_v1 isoforms and $Na_v1.4$ channels in different species (Figure 2A). F221S affects the fourth transmembrane α-helix of the first VSD of $Na_v1.4$, A715T affects the first α-helix of the pore domain in the DII, whereas F1419L and R1451H affect VSD-IV (Figure 2B,C). N1204D affects a pore-loop between α-helices of the pore domain III. Functional analysis showed that two variants, F221S and A715T, enhanced channel activation by shifting the voltage dependence of activation to more hyperpolarized voltages compared to the wild-type channel (Figure 3A–C, Table 3). Both variants affecting VSD-IV, F1419L and R1451H, accelerated the recovery from inactivation and the onset of closed state inactivation while slowing the open state inactivation and reducing the steepness of the slope of the voltage dependence of fast inactivation (Figure 3A,D–G, Table 3). Variant N1204D did not alter voltage dependencies or rates of state transitions but reduced current density (Figure 3A,B).

4 | Discussion

We report five *SCN4A* variants identified in patients presenting with various combinations of myotonia, myalgia, and muscle weakness, as well as myotonic discharges on EMG in most cases. Myalgia was absent only in patient F4 II:1 (F1419L). The symptoms were typically aggravated by physical exercise and/or cold, except for patient F7 II:1 (A715T). The findings are common in patients reported with other pathogenic *SCN4A* variants. Four of the variants showed GoF features strongly supporting the pathogenicity of the variants. N1204D was the only variant without myotonic discharges on EMG or enhanced channel function.

In general, symptoms were mild in all study patients resembling the phenotype resulting from *SCN4A* A1156T previously reported [10]. The facial muscles and the muscles in the upper limbs were more affected than the muscles in the lower limbs. This feature is common for patients with pathogenic *SCN4A* variants and myotonia [25, 26]. The condition of the female patients with the F221S variant deteriorated during pregnancies. This phenomenon has been reported in nondystrophic myotonic syndromes, also in conjunction with pathogenic *SCN4A* variants and in DM2 [14, 27, 28] (Trip, Drost, et al., 2009; Trivedi et al., 2013; Udd et al. 2012).

Common for all patients were myotonic discharges in EMG, except for the patient with N1204D. Only F4 II:1 and F5 II:1 had myotonic discharges in all the muscles examined. The findings were more distinct than what resulted from the *SCN4A* variant A1156T, although the phenotypes are similar [10].

Both F221S and A715T variants shifted the voltage dependence of activation to the hyperpolarizing direction. This GoF feature can account for the clinical manifestations and EMG findings in pedigrees F1, F5, F6, and F7. A variant homologous to F221S in $Na_v1.7$ has been identified in patients with erythermalgia (MichielsDrenth et al., 2005) [29]. Patch–clamp studies showed that the F216S variant similarly hyperpolarized the voltage dependence of activation (Choi et al., 2006) [30]. The same A715T variant has been identified before in sodium channel myotonia patients [19]. A different A715S variant in the same locus was discovered in patients with paramyotonia [31].

The patient with N1204D had symptomatic relatives in three consecutive generations. Symptoms were similar to those of the patients with A1156T [10]. Electrophysiological exercise testing was compatible with sodium channel disorder, although myotonic discharges were absent. The variant did not display any gain-of-function features but showed reduced current density. The tendency towards accelerated recovery, the main GoF feature of A1156T, did not reach significance in multiple comparison tests. $Na_v1.4$ loss-of-function variants have been associated with congenital myasthenia and congenital myopathy. They

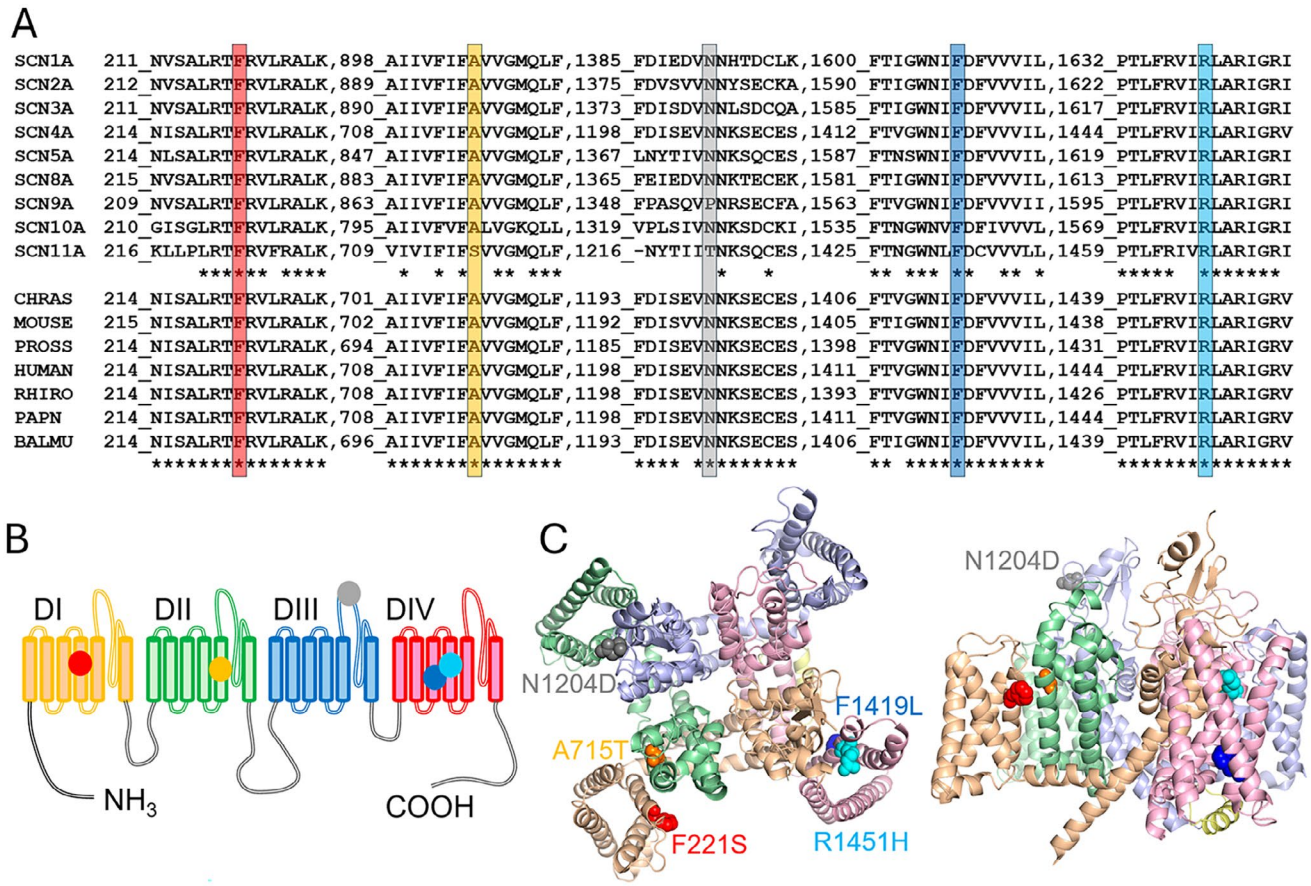

FIGURE 2 | Conservation and location of the variants in this study. (A) Alignment of human Na_V1 isoforms (top) and $Na_V1.4$ homologs across species (bottom) with asterisks indicating full conservation among the channels shown. F221S is indicated in red, A715T in orange, N1204D in gray, F1419L in blue, and R1451H in cyan boxes. Species include human, mouse, *Chrysochloris asiatica* (CHRAS) (Cape golden mole, Uniprot A0A9B0WHX8), *Prolemur simus* (PROSS) (Greater bamboo lemur, Uniprot A0A8C8ZD58), *Rhinopithecus roxellana* (RHIRO) (Golden snub-nosed monkey, Uniprot A0A2K6Q5D5), *Papio anubis* (PAPN) (Olive baboon, Uniprot A0A096NTU0), *Balaenoptera musculus* (BALMU) (Blue whale, Uniprot A0A8B8W847). (B–C) Location of the variants is indicated with filled circles in the topological scheme of Na_V1 channel (B) and in spheres in the 3D structure of $Na_V1.4$ channel (C) seen from above (left panel) and within (right panel) the membrane plane. In (B) DI–DIV indicate the number of the homologous repeat in Na_V1 structure. The repeats in (C) are color-coded as in (B) with voltage-sensing domains in the periphery and with the central pore domain.

typically show recessive inheritance, as heterozygous carriers are asymptomatic. The contribution of the loss-of-function features to clinical manifestations in pedigree F3 is thus not obvious and remains to be determined. Further genetic studies in and outside F3 may help to confirm the association of the N1204D variant with the condition.

Variants affecting VSD-IV, F1419L and R1451H, both showed similar GoF features by accelerating recovery from inactivation and decelerating onset of open state inactivation. These data are consistent with the clinical and EMG findings. Functional features of R1451H are qualitatively similar to those reported with the R1451L and R1451C variants found in families whose members had myotonia or periodic paralysis, while a homozygous carrier of R1451L experienced episodes of periodic paralysis triggered by hypokalemia [24, 32]. A different *SCN4A* variant c.4256 T > C p.(F1419S) has been reported in a family in which two members had hyperkalemic periodic paralysis [33]. A homologous p.(F1419L) variant causes equine hyperkalemic periodic paralysis in American Quarter Horses [34]. The channel inactivation was shown to be impaired, resulting in GoF feature [35].

The GoFs variants in this project showed small amplitude changes in channel function. Variants F221S and A715T showed a 4 mV change in voltage dependence of activation. F1419L and R1451H variants compromised inactivation by accelerating recovery and decelerating the onset of inactivation from the open state without effect on the voltage of half-maximal inactivation observed for the previously reported R1451L variant. These data align with mild clinical features of the patients discussed above. The onset of closed state inactivation was accelerated for both variants in VSD-IV. This is a LoF feature that results in faster reduction of channel availability following small depolarizations that do not reach the threshold of channel activation and may contribute to mild clinical features.

The functional data are also consistent with the stereotypical view of the effect pathogenic variants have on $Na_V1.4$ function,

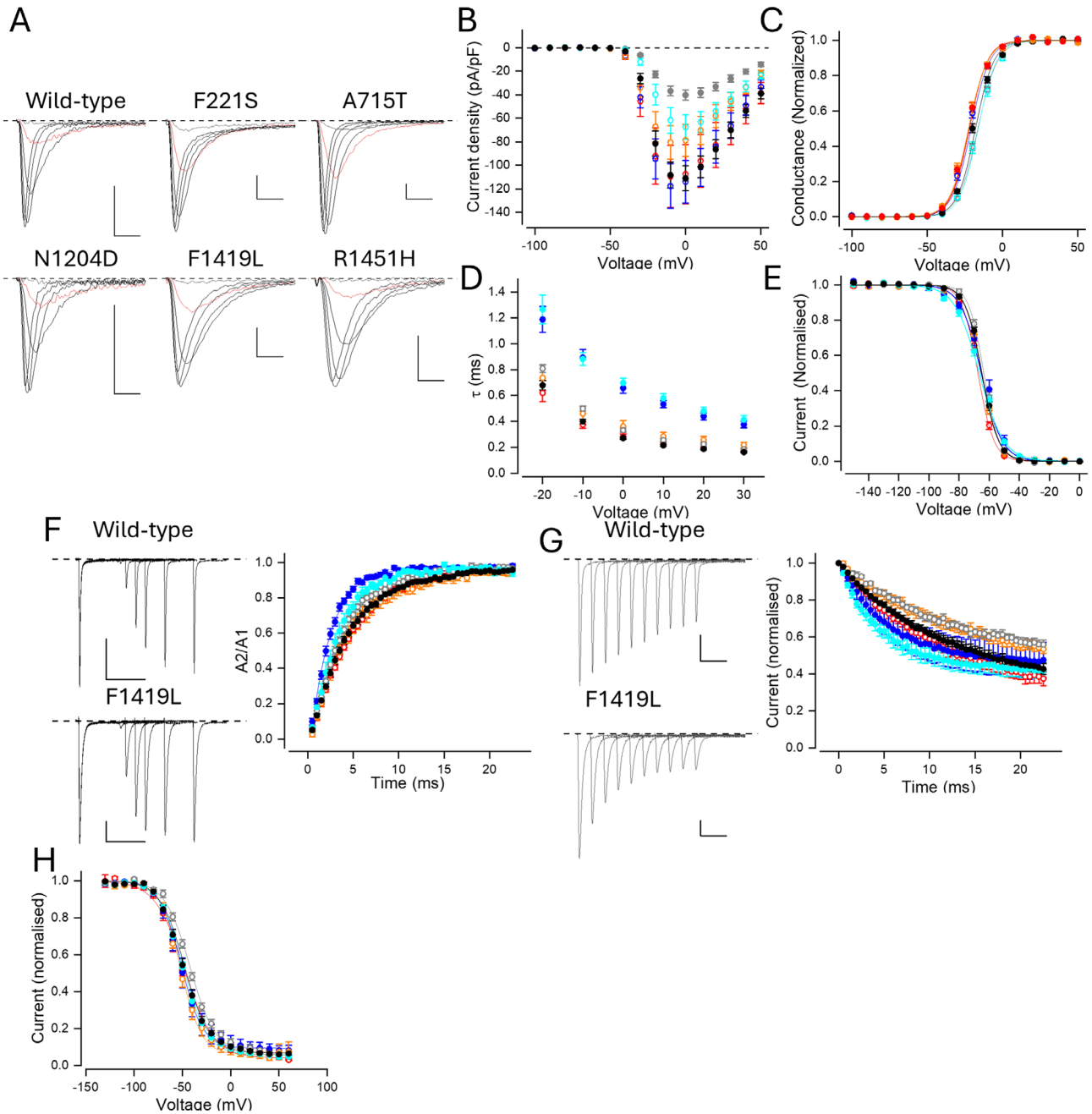

FIGURE 3 | Functional features of the variants in this study. Ms = millisecond; mV = millivolt; SEM = standard error of mean; Wild-type = WT. WT data is shown in black, F221S in red, A715T in orange, N1204D in gray, F1419L in blue, and R1451H in cyan. Data show mean ± SEM. Data with statistically significant differences to WT is shown in solid symbols (Table 3), and data with nonsignificant findings in open symbols. (A) Representative traces of the variants in response to voltage steps to voltages from −40 mV to 10 mV increments. Red traces show the current in response to the voltage step to −30 mV. Scale bars are 1 ms (x) and 1 nA (y). B-D. Peak current (B), peak conductance (C), and time constant of inactivation (D) in response to steps to indicated voltages are shown. Conductance was derived by dividing the current by V-V_{Rev}, where V_{Rev} is the reversal voltage of sodium. (E) Voltage dependence of fast inactivation is shown by plotting peak current in response to the voltage step to −10 mV following 150 ms prepulses to voltages indicated on the x-axis. (F) Representative currents (left panels) in response to two voltage pulses to 0 mV with currents in response to the first (10 ms) shown on the left of the trace. Current in response to the second pulse following recovery periods of 0, 0.5, 2, 4.5, 7, 12, and 19.5 ms at resting voltage is shown for WT (top) and F1419L (bottom). Scale bars are 10 ms (x) and 1 nA (y). The right panel plots peak current amplitude at the second pulse divided by the peak amplitude of the first pulse against the recovery time at holding voltage (A2/A1). (G) Representative currents (left panels) in response to voltage pulses to 0 mV following prepulse steps of increasing duration to −60 mV. Shown are current responses for 0, 2.5, 5, 7.5, 10, 12.5, 15, 17.5, 20, and 22.5 ms prepulses. Peak current amplitude against prepulse duration is shown in the right panel. Data are normalized to the amplitude of the first pulse (0 ms). (H) Voltage dependence of slow inactivation is shown by plotting peak current in response to the voltage step to −10 mV following 10 s prepulses to voltages indicated on the x-axis. Between pre- and test pulses, a 20 ms pulse to −100 mV is applied to allow recovery from fast inactivation. Data from individual cells were normalized to peak and bottom amplitudes of Boltzmann fit in (C and E) and to peak amplitude of Boltzmann fit in (H) Lines in (C, E and H) show the fit of the Boltzmann equation to the mean data.

TABLE 3 | Biophysical parameters of the $Na_V1.4$ variants in this study.

			A715T		F1419L		F221S		N1204D		R1451H		WT	
Activation	Current density	pA/pF	10	−110.4 ± 26.3	10	−118.0 ± 18.9	11	−82.1 ± 14.1	23	−40.5 ± 4.3***	13	−67.9 ± 10.5	35	−113.0 ± 10.9
	V(1/2)	mV		−23.0 ± 0.8*		−22.0 ± 0.7		−23.2 ± 0.8**		−16.6 ± 0.5		−16.2 ± 1.0		−19.1 ± 0.6
	V(Slope)	mV		6.5 ± 0.2		6.3 ± 0.1		6.8 ± 0.2		6.7 ± 0.2		6.8 ± 0.3		6.3 ± 0.2
Fast inactivation	V(1/2)	mV		−66.9 ± 0.6		−63.3 ± 1.6		−65.0 ± 0.4		−63.0 ± 0.6		−66.1 ± 0.9		−64.2 ± 0.6
	V(Slope)	mV		5.1 ± 0.1		7.0 ± 0.3***		5.6 ± 0.4		4.9 ± 0.2		8.3 ± 0.2***		5.1 ± 0.1
	τ onset @ 0 mV	ms		0.28 ± 0.02		0.66 ± 0.04***		0.36 ± 0.05		0.33 ± 0.01		0.70 ± 0.04***		0.27 ± 0.01
	τ onset @ −60 mV	ms	6	11.7 ± 0.7	6	5.8 ± 0.4**	5	15.8 ± 3.4	12	13.2 ± 0.8	8	5.0 ± 0.4***	20	11.6 ± 0.5
	τ recovery @ −80 mV	ms	9	4.8 ± 0.2	9	2.4 ± 0.1***	8	4.5 ± 0.6	17	3.6 ± 0.2	11	2.9 ± 0.2**	29	4.4 ± 0.2
Slow inactivation	V(1/2)	mV	4	−51.2 ± 2.8	6	−50.4 ± 3.8	4	−51.9 ± 1.9	11	−43.4 ± 0.9	7	−49.7 ± 1.3	17	−48.8 ± 1.7
	V(Slope)	mV		12.8 ± 0.2		10.7 ± 0.6		11.9 ± 1.3		12.4 ± 0.6		12.5 ± 0.3		12.3 ± 0.3

Note: Columns 1–3 indicate the parameter studied and the unit. The first column for each variant indicates the n of cells measured for this parameter, and the second column the mean ± SEM. Current density indicates maximum current density. Asterisks express p values: *$p < 0.05$, **$p < 0.01$, ***$p < 0.001$.

Abbreviations: ms, millisecond; mV, millivolt; pA, picoampere; pF, picofarad; SEM, standard error of mean; τ, time constant of onset or recovery from inactivation at mentioned voltages; V(1/2), mid-point voltage; V(Slope), slope factor; WT, wild-type.

as variants in the fourth repeat compromise channel inactivation, while variants in other domains predominantly enhance channel activation. Our data also suggest that the type of GoF feature, enhanced activation or attenuated inactivation, is not a key determinant of the mild clinical outcome in the current cohort. Finally, several voltage-gated sodium channel variants that disrupt channel activity are reported in the pore loops where N1204D is located [36], consistent with the reduced current density found in cells expressing this variant.

In conclusion, the clinical and functional data of four *SCN4A* variants described here suggest that they should be considered with patients complaining of exercise- and cold-induced myalgia and muscle stiffness, exertional myalgia, or exertional muscle cramping. While clinical data for the N1204D variant suggest a similar underlying mechanism, functional data indicate a distinct pathogenic mechanism. In cases without clinical myotonia, EMG can prove useful as it may reveal electrical myotonia. Electrophysiological exercise tests may also provide further evidence to support the diagnosis of a skeletal muscle channelopathy even if the genetic testing is unable to identify any previously known pathogenic gene variant.

Author Contributions

Vesa Periviita: writing – original draft, writing – review and editing, formal analysis, investigation, conceptualization. **Roope Männikkö:** writing – original draft, writing – review and editing, conceptualization, investigation, formal analysis, data curation. **Manu Jokela:** conceptualization, investigation, formal analysis. **Richa Sud:** investigation, data curation, formal analysis, conceptualization. **Michael G. Hanna:** supervision, formal analysis, conceptualization. **Bjarne Udd:** supervision, formal analysis, conceptualization, writing – review and editing. **Johanna Palmio:** writing – review and editing, supervision, conceptualization, investigation, formal analysis.

Conflicts of Interest

Bjarne Udd and Johanna Palmio are members of the European Reference Network for Rare Neuromuscular Diseases (ERN EURO-NMD).

Data Availability Statement

The data that support the findings of this study are available on request from the corresponding author. The data are not publicly available due to privacy or ethical restrictions.

References

1. S. C. Cannon, "Sodium Channelopathies of Skeletal Muscle," *Handbook of Experimental Pharmacology* 246 (2018): 309–330, https://doi.org/10.1007/164_2017_52.

2. M. DiFranco and J. L. Vergara, "The Na Conductance in the Sarcolemma and the Transverse Tubular System Membranes of Mammalian Skeletal Muscle Fibers," *Journal of General Physiology* 138, no. 4 (2011): 393–419, https://doi.org/10.1085/jgp.201110682.

3. W. A. Catterall, M. J. Lenaeus, and T. M. Gamal El-Din, "Structure and Pharmacology of Voltage-Gated Sodium and Calcium Channels," *Annual Review of Pharmacology and Toxicology* 60 (2020): 133–154, https://doi.org/10.1146/annurev-pharmtox-010818-021757.

4. P. Imbrici, A. Liantonio, G. M. Camerino, et al., "Therapeutic Approaches to Genetic Ion Channelopathies and Perspectives in Drug Discovery," *Frontiers in Pharmacology* 7 (2016): 121, https://doi.org/10.3389/fphar.2016.00121.

5. W. Huang, M. Liu, S. F. Yan, and N. Yan, "Structure-Based Assessment of Disease-Related Mutations in Human Voltage-Gated Sodium Channels," *Protein & Cell* 8, no. 6 (2017): 401–438, https://doi.org/10.1007/s13238-017-0372-z.

6. K. Jurkat-Rott, N. Mitrovic, C. Hang, et al., "Voltage-Sensor Sodium Channel Mutations Cause Hypokalemic Periodic Paralysis Type 2 by Enhanced Inactivation and Reduced Current," *Proceedings of the National Academy of Sciences of the United States of America* 97, no. 17 (2000): 9549–9554, https://doi.org/10.1073/PNAS.97.17.9549.

7. K. Jurkat-Rott and F. Lehmann-Horn, "Genotype–Phenotype Correlation and Therapeutic Rationale in Hyperkalemic Periodic Paralysis," *Neurotherapeutics* 4, no. 2 (2007): 216–224, https://doi.org/10.1016/j.nurt.2007.02.001.

8. L. J. Ptáček, A. L. George, R. L. Barchi, et al., "Mutations in an S4 Segment of the Adult Skeletal Muscle Sodium Channel Cause Paramyotonia Congenita," *Neuron* 8, no. 5 (1992): 891–897, https://doi.org/10.1016/0896-6273(92)90203-P.

9. H. Lerche, R. Heine, U. Pika, et al., "Human Sodium Channel Myotonia: Slowed Channel Inactivation due to Substitutions for a Glycine Within the III-IV Linker," *Journal of Physiology* 470, no. 1 (1993): 13–22, https://doi.org/10.1113/jphysiol.1993.sp019843.

10. J. Palmio, S. Sandell, M. G. Hanna, R. Mannikko, S. Penttila, and B. Udd, "Predominantly Myalgic Phenotype Caused by the c.3466G > A p.A1156T Mutation in SCN4A Gene," *Neurology* 88, no. 16 (2017): 1520–1527, https://doi.org/10.1212/WNL.0000000000003846.

11. A. Tsujino, C. Maertenst, K. Ohno, et al., "Myasthenic Syndrome Caused by Mutation of the SCN4A Sodium Channel," *Proceedings of the National Academy of Sciences of the United States of America* 100, no. 12 (2003): 7377–7382, https://doi.org/10.1073/PNAS.1230273100.

12. I. T. Zaharieva, M. G. Thor, E. C. Oates, et al., "Loss-Of-Function Mutations in SCN4A Cause Severe Foetal Hypokinesia or 'Classical' Congenital Myopathy," *Brain* 139, no. 3 (2016): 674–691, https://doi.org/10.1093/BRAIN/AWV352.

13. A. Todd, C. L. McNamara, M. Balaj, et al., "The European Epidemic: Pain Prevalence and Socioeconomic Inequalities in Pain Across 19 European Countries," *European Journal of Pain* 23, no. 8 (2019): 1425–1436, https://doi.org/10.1002/EJP.1409.

14. B. Udd and R. Krahe, "The Myotonic Dystrophies: Molecular, Clinical, and Therapeutic Challenges," *Lancet Neurology* 11, no. 10 (2012): 891–905, https://doi.org/10.1016/S1474-4422(12)70204-1.

15. K. Suetterlin, R. Mannikko, and M. G. Hanna, "Muscle Channelopathies: Recent Advances in Genetics, Pathophysiology and Therapy," *Current Opinion in Neurology* 27, no. 5 (2014): 583–590, https://doi.org/10.1097/WCO.0000000000000127.

16. J. Trip, J. de Vries, G. Drost, H. B. Ginjaar, B. G. van Engelen, and C. G. Faber, "Health Status in Non-Dystrophic Myotonias: Close Relation With Pain and Fatigue," *Journal of Neurology* 256, no. 6 (2009): 939–947, https://doi.org/10.1007/s00415-009-5049-y.

17. K. Suokas, J. Palmio, S. Sandell, B. Udd, and A. Hietaharju, "Pain in SCN4A Mutated P.A1156T Muscle Sodium Channelopathy-A Postal Survey," *Muscle & Nerve* 57, no. 6 (2018): 1014–1017, https://doi.org/10.1002/mus.26050.

18. V. Periviita, J. Palmio, M. Jokela, et al., "CACNA1S Variant Associated With a Myalgic Myopathy Phenotype," *Neurology* 101, no. 18 (2023): e1779–e1786, https://doi.org/10.1212/WNL.0000000000207639.

19. E. Fournier, K. Viala, H. Gervais, et al., "Cold Extends Electromyography Distinction Between Ion Channel Mutations Causing Myotonia," *Annals of Neurology* 60, no. 3 (2006): 356–365, https://doi.org/10.1002/ana.20905.

20. E. Fournier, M. Arzel, D. Sternberg, et al., "Electromyography Guides Toward Subgroups of Mutations in Muscle Channelopathies," *Annals of Neurology* 56, no. 5 (2004): 650–661, https://doi.org/10.1002/ana.20241.

21. B. Udd, W. Stenzel, A. Oldfors, et al., "1st ENMC European Meeting: The EURO-NMD Pathology Working Group Recommended Standards for Muscle Pathology Amsterdam, the Netherlands, 7 December 2018," *Neuromuscular Disorders* 29, no. 6 (2019): 483–485, https://doi.org/10.1016/j.nmd.2019.03.002.

22. O. Raheem, S. Huovinen, T. Suominen, H. Haapasalo, and B. Udd, "Novel Myosin Heavy Chain Immunohistochemical Double Staining Developed for the Routine Diagnostic Separation of I, IIA and IIX Fibers," *Acta Neuropathologica* 119, no. 4 (2010): 495–500, https://doi.org/10.1007/s00401-010-0643-8.

23. A. Evila, M. Arumilli, B. Udd, and P. Hackman, "Targeted Next-Generation Sequencing Assay for Detection of Mutations in Primary Myopathies," *Neuromuscular Disorders* 26, no. 1 (2016): 7–15, https://doi.org/10.1016/j.nmd.2015.10.003.

24. S. Luo, M. Sampedro Castañeda, E. Matthews, et al., "Hypokalaemic Periodic Paralysis and Myotonia in a Patient With Homozygous Mutation p.R1451L in Na(V)1.4," *Scientific Reports* 8, no. 1 (2018): 9712–9714, https://doi.org/10.1038/s41598-018-27822-2.

25. E. Matthews, D. Fialho, S. V. Tan, et al., "The Non-Dystrophic Myotonias: Molecular Pathogenesis, Diagnosis and Treatment," *Brain* 133, no. 1 (2010): 9–22, https://doi.org/10.1093/brain/awp294.

26. R. J. Barohn, M. M. Dimachkie, and C. E. Jackson, "A Pattern Recognition Approach to Patients With a Suspected Myopathy," *Neurologic Clinics* 32, no. 3 (2014): 569–593, vii, https://doi.org/10.1016/j.ncl.2014.04.008.

27. J. Trip, G. Drost, H. B. Ginjaar, et al., "Redefining the Clinical Phenotypes of Non-Dystrophic Myotonic Syndromes," *Journal of Neurology, Neurosurgery, and Psychiatry* 80, no. 6 (2009): 647–652, https://doi.org/10.1136/jnnp.2008.162396.

28. J. R. Trivedi, B. Bundy, J. Statland, et al., "Non-Dystrophic Myotonia: Prospective Study of Objective and Patient Reported Outcomes," *Brain* 136, no. 7 (2013): 2189–2200, https://doi.org/10.1093/brain/awt133.

29. J. P. Drenth, R. H. te Morsche, G. Guillet, A. Taieb, R. L. Kirby, and J. B. Jansen, "SCN9A Mutations Define Primary Erythermalgia as a Neuropathic Disorder of Voltage Gated Sodium Channels," *Journal of Investigative Dermatology* 124, no. 6 (2005): 1333–1338.

30. J.-S. Choi, S. D. Dib-Hajj, and S. G. Waxman, "Inherited erythermalgia: Limb pain from an S4 charge-neutral Na channelopathy," *Neurology* 67, no. 9 (2006): 1563–1567, https://doi.org/10.1212/01.wnl.0000231514.33603.1e.

31. M. J. Mazón, F. Barros, P. De la Peña, et al., "Screening for Mutations in Spanish Families With Myotonia. Functional Analysis of Novel Mutations in CLCN1 Gene," *Neuromuscular Disorders* 22, no. 3 (2012): 231–243, https://doi.org/10.1016/j.nmd.2011.10.013.

32. H. Poulin, P. Gosselin-Badaroudine, S. Vicart, et al., "Substitutions of the S4DIV R2 Residue (R1451) in NaV1.4 Lead to Complex Forms of Paramyotonia Congenita and Periodic Paralyses," *Scientific Reports* 8, no. 1 (2018): 1–13, https://doi.org/10.1038/s41598-018-20,468-0.

33. B. C. Stunnenberg, J. Raaphorst, J. C. W. Deenen, et al., "Prevalence and Mutation Spectrum of Skeletal Muscle Channelopathies in The Netherlands," *Neuromuscular Disorders* 28, no. 5 (2018): 402–407, https://doi.org/10.1016/J.NMD.2018.03.006.

34. J. A. Rudolph, S. J. Spier, G. Byrns, C. V. Rojas, D. Bernoco, and E. P. Hoffman, "Periodic Paralysis in Quarter Horses: A Sodium Channel Mutation Disseminated by Selective Breeding," *Nature Genetics* 2, no. 2 (1992): 144–147, https://doi.org/10.1038/ng1092-144.

35. S. Cannon, L. Hayward, J. Beech, and R. Brown, "Sodium Channel Inactivation Is Impaired in Equine Hyperkalemic Periodic Paralysis," *Journal of Neurophysiology* 73, no. 5 (1995): 1892–1899, https://doi.org/10.1152/jn.1995.73.5.1892.

36. A. Brunklaus, T. Feng, T. Brünger, et al., "Gene Variant Effects Across Sodium Channelopathies Predict Function and Guide Precision Therapy," *Brain* 145, no. 12 (2022): 4275–4286, https://doi.org/10.1093/BRAIN/AWAC006.